Check for updates

View Article Online
View Journal

Dalton Transactions

Accepted Manuscript

This article can be cited before page numbers have been issued, to do this please use: A. Mahammad, M. Debnath, M. Dolai, K. Pal, S. Bhunya, A. Paul and H. M. Lee, *Dalton Trans.*, 2018, DOI: 10.1039/C7DT04718E.

This is an Accepted Manuscript, which has been through the Royal Society of Chemistry peer review process and has been accepted for publication.

Accepted Manuscripts are published online shortly after acceptance, before technical editing, formatting and proof reading. Using this free service, authors can make their results available to the community, in citable form, before we publish the edited article. We will replace this Accepted Manuscript with the edited and formatted Advance Article as soon as it is available.

You can find more information about Accepted Manuscripts in the author guidelines.

Please note that technical editing may introduce minor changes to the text and/or graphics, which may alter content. The journal's standard Terms & Conditions and the ethical guidelines, outlined in our author and reviewer resource centre, still apply. In no event shall the Royal Society of Chemistry be held responsible for any errors or omissions in this Accepted Manuscript or any consequences arising from the use of any information it contains.

ROYAL SOCIETY OF CHEMISTRY

rsc.li/dalton

View Article Online
CREATED USING THE RSC ARTICLE TEMPLATE - SEE WWW.RSC.ORG/ELECTRONICFILES FOR FURTHER DETAILS DOI: 10.1039/C7DT04718E

Published on 22 January 2018. Downloaded by University of Reading on 24/01/2018 07:27:54.

Mono- and dinuclear oxidovanadium(V) complexes of an amine-bis(phenolate) ligand with bromo-peroxidase activities: synthesis, characterization, catalytic, kinetic and computational studies

Mainak Debnath[a], Malay Dolai[a], Kaberi Pal[a], Sourav Bhunya[b], Akan Paul[b], Hon Man Lee[c] and Mahammad Ali[a,*]

[a]*Department of Chemistry,Jadavpur University, 188, Raja Subodh Chandra Mullick Rd, Kolkata, West Bengal 700032, India, E-mail: m_ali2062@yahoo.com;*
[b]*Raman Centre for Atomic,Optical and Molecular Physics, Indian Association for the Cultivation of Science, Jadavpur, Kolkata-700032, India*
[c]*Department of Chemistry, National Changhua University of Education, Changhua, Taiwan 50058*

This submission was created using the RSC Article Template (DO NOT DELETE THIS TEXT)
(LINE INCLUDED FOR SPACING ONLY - DO NOT DELETE THIS TEXT)

Abstract

Mono and dinuclear oxidovanadium(V) complexes $[V^{V}O(L^{1})(Cl)]$ (**1**) and $[L^{1}V^{V}O(\mu_2\text{-}O)VO(L^{1})]$ (**2**) of ONNO donor amine-bis(phenolate) ligand (H_2L^1) have been readily synthesized by the reaction between H_2L^1 and $VCl_3.(THF)_3$ or $VO(acac)_2$ in MeOH or MeCN respectively and characterized by mass spectroscopy,^{1}H-NMR and FTIR study. Both the complexes possess distorted octahedral geometry around each V center. On addition of 1 equivalent or more acid to MeCN solution of complex **1** it immediately turned into the protonated form which might be in equilibrium as: $[L^{1}ClV^{V}{=}OH]^{+} \longleftrightarrow [L^{1}ClV^{V}\text{–}OH]^{+}$ (in case of $[L^{1}ClV^{V}{=}OH]^{+}$ oxo-O is just protonated whereas in $[L^{1}ClV^{V}\text{–}OH]^{+}$ it is hydroxo species), with the shift in λ_{max} from 610 nm to 765 nm. Similar is the case for complex **2**. The complexes **1** and **2** are efficient to catalyze the oxidative bromination of salicylaldehyde in the presence of H_2O_2 to produce 5-bromo salicylaldehyde as the major product with TONs 405 and 450, respectively in the mixed solvent system (H_2O: MeOH: THF = 4: 3: 2, v/v). The kinetic analysis of the bromide oxidation reaction indicates a mechanism which is first order in protonated peroxidovanadium complex and bromide ion and limiting first-order on $[H^+]$. The evaluated k^{Br} and k^{H} values are 5.78 ± 0.20 and 11.01 ± 0.50 $M^{-1}s^{-1}$ for complex **1** and 6.21 ± 0.13 and 20.14 ± 0.72 $M^{-1}s^{-1}$ for complex **2**, respectively. The kinetic and thermodynamic acidities of protonated oxido species of complexes **1** and **2** are:pK_a = 2.55 (2.35) and 2.16 (2.19), respectively which are far more acidic than those reported by Pecoraro *et. al*. for peroxido-protonation instead of oxido protonation. On the basis of chemistry observed for these model compounds, a mechanism of halide oxidation and a detailed catalytic cycle are proposed for the vanadium haloperoxidase enzyme and substantiated by detail DFT calculations.

.

Introduction

In recent years, the roles of vanadium in the biosphere have become an interesting topic of research. Vanadium occurs naturally in amavadin, a compound isolated from mushroom *Amanita muscaria* and similar species. It is found in high concentrations in ascidians and is known to be essential for the function of certain types of nitrogenase and haloperoxidase enzymes.[1] In addition, vanadium ions and their compounds are known to be potent insulin mimics and as such, may find use as alternatives to insulin in the treatment of diabetes.[2]

The vanadate dependent haloperoxidases (VHPOs) are the enzymes that catalyze the $2e^-$ oxidation of a halide by H_2O_2 to the corresponding hypohalaous acids, HOX. Thereby, the formed HOX reacts with a broad range of organic substrates to form a diverse variety of halogenated compounds. The classification of VHPOs is based on the nature of halides oxidized. When it catalyses the oxidation of Cl^-, Br^- or I^- in the presence of H_2O_2 it is designated as a chloroperoxidaes (CPOs), oxidation of Br^- or I^- as bromoperoxidases (BPOs) or oxidation of I^- as iodoperoxidases (IPOs). This distinction is however sometimes arbitrary. A variety of halogenated organic compounds, ranging from simple volatile halohydrocarbons (pollutants in the atmosphere)[3,4] to relatively complicated chiral structures (antibiotics),[5] is believed to be the natural products of the vanadium haloperoxidases. BPOs, found in red and brown seaweeds or terrestrial fungi, have been shown to catalyze the bromination of various organic substrates including 2-chloro-5,5-dimethyl-1,3-cyclohexane-dione (mcd), the standard substrate for the determination of haloperoxidase activity using H_2O_2 as the oxidant.[6] Otherwise, singlet oxygen[7] is formed in the absence of any nucleophilic acceptor. This disproportionation reaction of hydrogen peroxide is a bromide-mediated reaction, i.e. V-BPO does not catalyze the formation of singlet oxygen in the absence of bromide ion. As for an example, at pH 6.5 using 2 mM hydrogen peroxide, 0.1 M bromide and 50 mM mcd, the

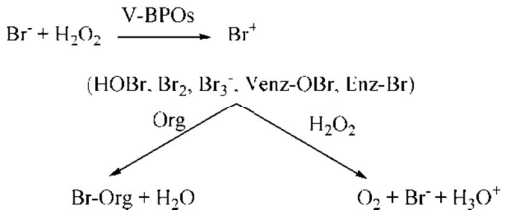

Scheme-1

specific activity of Ascophyllum nodosum towards bromination of mcd is 170 U mg^{-1}.[8] A common intermediate ('Br^+') is likely

Dalton Transactions Accepted Manuscript

View Article Online
CREATED USING THE RSC ARTICLE TEMPLATE - SEE WWW.RSC.ORG/ELECTRONICFILES FOR FURTHER DETAILS DOI: 10.1039/C7DT04718E

Published on 22 January 2018. Downloaded by University of Reading on 24/01/2018 07:27:54.

to exist which is formed in a rate determining step and which is responsible for both the generation of singlet dioxygen through oxidation of an additional equivalent of hydrogen peroxide and brominated products (see Scheme-1).[7,9-11]

The structure of vanadium haloperoxidase shows that the vanadium ion is ligated to the protein backbone via one histidine nitrogen donor atom, whilst the oxido moieties are strongly H-bonded to arginine, lysine, histidine and serine amino acids[12] (see Fig. 1 for a schematic representation).

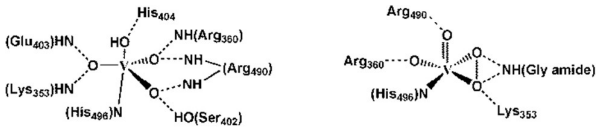

Native site Peroxo site

Fig. 1.The native and peroxidovanadium site in V-CPOs[12]

Various model systems of vanadium were designed in order to examine which structural features are important for the catalytic properties of these enzymes[13,14] where vanadium is either in the +4 [15-17] or +5 oxidation state.[18-21] A great variety of vanadium compounds have been studied as functional models for V-haloperoxidases to get a better understanding of the working mechanism of the vanadium haloperoxidase enzyme and to determine the role of vanadium.[12] The first reported functional mimic of V-BPO is *cis*-dioxidovanadium(V) (VO_2^+) in acidic aqueous solution,[22,23] which catalyzes the bromination of 1,3,5-trimethoxybenzene (TMB) as well as the bromide-mediated disproportionation of H_2O_2. Nevertheless, the exact nature of this halogenating intermediate has not been determined as yet. All these prompted us to design and synthesize structural and functional models of the biomolecules, which has the potential ability to catalyze the bromination of organic substrate in order to get a better understanding of the mechanism of such reactions. For some time, we have been interested in the chemistry vanadium compounds with amine *bis*-phenolate ligands that showed interesting catalytic activities towards hydrocarbon oxidation and epoxidation reactions.[24-27] We will reveal here the structures of two vanadium complexes, one mononuclear (**1**) and another one is oxido-bridged dinuclear (**2**) complex of N_2O_2 donor amine-bisphenolate ligand (Scheme 2) that showed interesting bromoperoxidase activity towards the bromination of salicylaldehyde. The model complexes described here, are indeed able to catalyze the bromination of salicylaldehyde. Not only that, though some of the complexes with one weak V-O bond from water or alcohol are reported[12] there is no single report on such complexes having V-Cl bond which may easily be dissociated to provide an additional coordination site for a substrate (H_2O_2).

Experimental Section

Physical Measurements

Elemental analyses were carried out using a Perkin-Elmer 240 elemental analyser. Infrared spectra (400–4000 cm^{-1}) were recorded from KBr pellets on a Nicolet Magna IR 750 series-II FTIR spectrophotometer. Electronic spectra were recorded from Agilent 8453 UV–Vis diode-array spectrophotometer.Mass spectra were recorded on a HRMS (model XEVO G2QTof) spectrometer with electron spray ionization source in MeCN. Electrochemical measurements were carried out using a computer controlled AUTOLAB (Model: AutoLab 302) cyclic voltammeter with platinum working electrode, platinum-wire counter electrode and saturated calomel (SCE) reference electrode in MeCN using tetrabutylammonium perchlorate as supporting electrolyte. ^{1}H-NMR spectra were recorded in $CDCl_3$, on a Bruker 300 MHz NMR spectrometer using tetramethylsilane (δ = 0) as an internal standard.

DFT calculations

All theoretical calculations were conducted using standard Gaussian09 package[28]. We have optimized each intermediate and transition states in gas phase using B3LYP[29] functional in conjunction with Pople's 6-31G(d) basis set on all atoms except Vanadium. Vanadium was described by the LANL2DZ basis set which is a combination of effective core potential LANL2 and a valence double-ξ basis set. Each intermediate were characterized by the presence of all real modes. Transition states were identified by the presence of all real modes barring one imaginary mode by harmonic frequency analysis of the optimized structures. Solvent effects were included in energy along the reaction pathways by performing single point calculations within the SMD solvent model[30] and water as solvent using 6-31^{++}g(d,p) basis set for each atom except vanadium which was described by the same basis set used for gas phase optimization. The solution phase free energies of each species were estimated by considering the suppression of translational entropy due to transfer from gas phase to solution phase. We have considered the decrease in entropies as 0.5 times of total entropies which is based on the experimental works of Wertz.[31] This empirical approach for obtaining solvent phase entropic corrections from ideal gas model based computed gas phase entropies has been widely used as was used in other density functional studies of reaction mechanisms. [32]

Materials

Starting materials for the synthesis of the ligand (H_2L^1) and complexes (**1** and **2**) namely, 2,4-di-*tert*-butylphenol (Aldrich), 2-aminomethylpyridine (Aldrich), formaldehyde (Merck India), VCl_3.$(THF)_3$ (Aldrich), [VO(acac)$_2$] (Lancaster India) were of reagent grade and used as received. Solvents like methanol, ethanol, acetonitrile (Merck India) were of reagent grade and dried by standard methods before use. Substrates namely salicylaldehyde (Aldrich) used in the catalytic reactions is of reagent grade and used as received. 30% H_2O_2 (Merck India), KBr (Merck India) and 70% $HClO_4$ (Aldrich) were used in the catalytic bromination reactions.

Synthesis of amine-*bis*(phenolate) ligand (H_2L^1)

The ligand (H_2L^1) has been synthesized according to a reported method[33] and characterized by CHN analysis.

H_2L^1: Yield 85%. *Ana. Cal.* values for Molecular formula, $C_{36}H_{52}N_2O_2$ C, 79.36%; H, 9.62%; N,5.14%; *Found* C ,79.72%; H 9.45%; N, 5.46%. ^{1}H-NMR 1.28 (s, 36-H); 3.11 (d, 2-H); 3.73 (s, 4-H); 6.87-7.26 (m, 6-ArH); 7.57 (t, 1-ArH); 8.688 (d, 1-ArH); 9.55 (b, -OH protons) (Fig. S1)

Preparation of complexes

Dalton Transactions Accepted Manuscript

View Article Online
CREATED USING THE RSC ARTICLE TEMPLATE - SEE WWW.RSC.ORG/ELECTRONICFILES FOR FURTHER DETAILS DOI: 10.1039/C7DT04718E

Published on 22 January 2018. Downloaded by University of Reading on 24/01/2018 07:27:54.

Synthesis of [VO(L^1)Cl] (1)

1.0 mmol (0.544 g) of the ligand H_2L^1 was dissolved in 20 mL MeOH and refluxed with 2 mmol (0.202 g) TEA (triethylamine) for 10 minutes. The solution was then cooled. A solution of $VCl_3.(THF)_3$ (1 mmol, 0.374 g) in MeOH was added drop wise to the above ligand solution and the resulting mixture was refluxed for 2 hours. The dark blue solution was filtered off after cooling to room temperature and the filtrate was subjected to slow evaporation at room temperature. Dark blue block shaped single crystals were obtained in 2 days.

[VO(L^1)Cl]: Yield 70%. *Ana. Cal* value for Molecular formula, $C_{36}H_{50}ClN_2O_3V$ C, 67.02%; H, 7.81%; N,4.34%; *Found* C, 66.97%; H, 7.79%; N, 4.32%. FTIR (KBr disc; cm^{-1}) *ν*(V=O) 975 (Fig. S2). ^{1}H-NMR 1.25-1.61 (m, 36-H); 3.10 (s, 2-H); 3.43 (t, 2-H); 3.56 (t, 2-H); 6.58-7.28 (m, 8-ArH) (Fig. S3). ESI-MS$^+$: ([L^{1}VO]$^+$) 609.3953 (Fig. S4).

Synthesis of [{VO(L^1)}$_2$O] (2)

1.0 mmol (0.544 g) of the ligand H_2L^1 was dissolved in 20 mL MeCN and was refluxed with 2 mmol (0.202 g) TEA for 10 minutes. The solution was then cooled. A solution of $[VO(acac)_2]$ (1 mmol, 0.265 g) in MeCN was added drop wise to the previous ligand solution and the resulting mixture was refluxed for 3 hours. The dark blue solution was filtered off after cooling to room temperature and the filtrate was subjected to slow evaporation at room temperature whereupon dark blue block shaped single crystals suitable for X-ray study were obtained within 3 days.

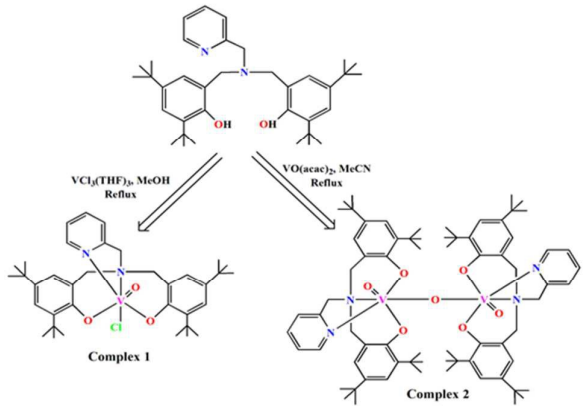

Scheme-2.Synthetic routes for complexes **1** and **2**.

[{VO(L^1)}$_2$O].Yield 73%. *Ana. Cal.*value for Molecular formula, $C_{72}H_{100}N_4O_7V_2$ C, 69.997%; H, 8.16%; N, 4.54%; *Found* C, 70.00 %; H, 8.11%; N, 4.49%. FTIR (KBr disc; cm^{-1}) *ν*(V=O) 975 and *ν*(V-O-V) 759 (Fig. S5). ^{1}H-NMR 1.14-2.00 (m, 72-H); 3.49-3.80 (m, 8-H); 5.63-5.67 (m, 4-H); 6.66-8.99 m, 16-ArH) (Fig. S6). ESI-MS$^+$: ([L^{1}VO(μ$_2$-O)VOL^1]) 1235.8259 (Fig. S7).

X-Ray Crystallography

Intensity data of the complex **1** were collected at 150K on a smart CCD diffractometer with the *ω*−2*θ* scan mode. The intensities were corrected for Lorentz and polarization effects and for absorption using the *ψ-scan* method. But, for complex **2,** X-ray data collection of the single crystal was performed at 150K using Bruker APEX II diffractometer, equipped with a normal focus, sealed tube X-ray source with graphite mono-chromated MoK_α radiation (λ= 0.71073Å). All the structures were solved by SHELXS-14[34] using Patterson method and followed by successive Fourier and difference Fourier map. Full matrix least-squares refinements were performed on F^2 using SHELXL-14[34] with anisotropic displacement parameters for all non-hydrogen atoms. All the hydrogen atoms were fixed geometrically by HFIX command and placed in their ideal positions. We restrain ourselves from reporting the data of complexes **1** and **2** as the data were of very poor quality even after several trials.

Experimental setup for catalytic bromination

A general procedure was applied to all reactions. A representative substrate, namely salicylaldehyde (20 mmol), was dissolved in a mixed solvent (H_2O: MeOH: THF = 4: 3: 2)[35] and the resulting solution was taken in a 50 mL capacity round bottom flask. To the above solution was then added KBr (40 mmol) followed by 2 ml (67 mmol) of 30% H_2O_2.
An appropriate catalyst (say, complex **1)** (0.026 g, 0.04 mmol) and 70% $HClO_4$ (0.10 ml) were added and the reaction was considered to begin with stirring. After 2 h of stirring at ambient temperature 0.1 ml of 70% $HClO_4$ was further added and stirring was continued for next 12 h. The separated white product was filtered, washed with water, followed by diethyl ether and dried in air. The crude mass was dissolved in CH_2Cl_2 and insoluble material was separated by filtration. After evaporation of the solvent to *ca.* 5 ml it was loaded over the column packed with silica gel. The fast moving band on elution with CH_2Cl_2 was collected and evaporated to dryness to give 5-bromo-salicylaldehyde.

Results and Discussion

Syntheses

Tetradenate N_2O_2 donor ligand H_2L^1 was synthesized by simple Mannich condensation of 2-aminomethylpyridine with 2,4-ditertiarybutylphenol and formaldehyde in MeOH. Straight forward reactions of this ligand with one equivalent of either $VCl_3(THF)_3$ in MeOH or $[VO(acac)_2]$ in MeCN under reflux in presence of two equivalents of TEA lead to complexes **1** and **2**, respectively.

The single crystal X-ray diffraction studies showed that both the complexes **1** and **2** crystallize in the monoclinic system with space group P21/c. As the diffraction data are not of good quality, only the molecular views of compounds **1** and **2** (Fig.2 and 3) are provided to show the connectivity and coordination environment of the complexes.

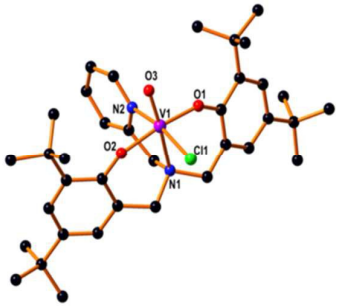

Fig. 2. Molecular view of complex **1**; H atoms are omitted for clarity.

Dalton Transactions Accepted Manuscript

View Article Online
CREATED USING THE RSC ARTICLE TEMPLATE - SEE WWW.RSC.ORG/ELECTRONICFILES FOR FURTHER DETAILS DOI: 10.1039/C7DT04718E

Published on 22 January 2018. Downloaded by University of Reading on 24/01/2018 07:27:54.

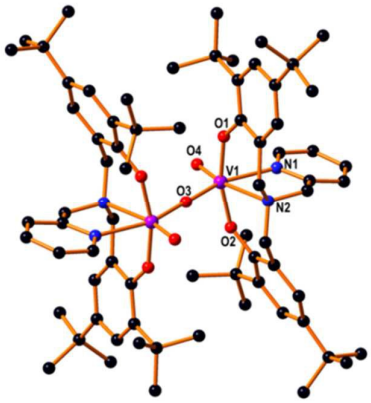

Fig. 3. Molecular view of complex **2**; H atoms are omitted for clarity.

Electrochemical study

The electrochemical behaviors of complexes were studied by cyclic Voltammetry in the range +1.5 to -1.5V at a scan rate 100 mVs^{-1} in MeCN on glassy carbon versus SCE using tetrabutylammonium perchlorate (TBAPC) as the supporting electrolyte. The cyclic voltammogram for complex **1** (Fig. 4) was found to be quasi-reversible in nature with $E_{1/2}$ = 0. 385V (E_{pa} = 0.444V, E_{pc} = 0.326V) and ΔE= 0.118V. The complex **2** remains as a dinuclear entity in solution as evidenced from HRMS spectrum (Fig. S7). The two peaks (Fig. 4) at -0.422 (not well resolved) and -0.892 V correspond to V(V)-V(V)→ V(V)-V(IV) and V(V)-V(IV)→ V(IV)-V(IV) reductions while the other peaks at -0.497 and 0.918V correspond to V(IV)-V(IV)→ V(IV)-V(V) and V(IV)-V(V)→ V(V)-V(V) oxidations. The $E_{½}$ = -0.657V corresponds to V(V)-V(IV) ⇌ V(IV)-V(IV) process and $E_{½}$ = 0.2105V corresponds to V(IV)-V(V) ⇌ V(V)-V(V) process. The redox couple V(V)-V(IV)/V(IV)-V(IV) appears to be quasi reversible whereas, the other redox couple V(IV)-V(V)/V(V)-V(V) appears to be irreversible in nature. Controlled coulometric experiment shows that the wave is one electron transfer process. Since the phenolate ligand as well as methoxy group could not be reduced in this potential range[36], we assign them as metal centred reduction potentials for the VO^{3+}/VO^{2+} couple.

It is interesting to note that, a considerable shift in the peak positions of the CV for both the complexes in the presence of small amount (≤ 1.0 x 10^{-3} M) of perchloric acid, were observed. For complex **1**, E_{pa} and E_{pc} are shifted from 0.444V to 0.630V and from 0.326V to 0.206V (Fig. S8), respectively. In case of complex **2** only two peaks (Fig. S8) were observed with E_{pa} 0.466V and E_{pc} 0.290V. This may be attributed to the formation of mononuclear protonated species of the corresponding complexes in the presence of 1.0 x 10^{-3} M $HClO_4$.

Electronic Spectra

Absorption spectrum of complex **1** shows single peak at 619 nm (ε/ $M^{-1}cm^{-1}$ = 2400) whereas complex **2** shows single peak at 603 nm (ε/ $M^{-1}cm^{-1}$ = 3100). Both the spectra of complexes **1** and **2** may arise due to the ligand (Phenoxido) to metal [V(V)] charge transfer (LMCT) transitions (Fig. S9).

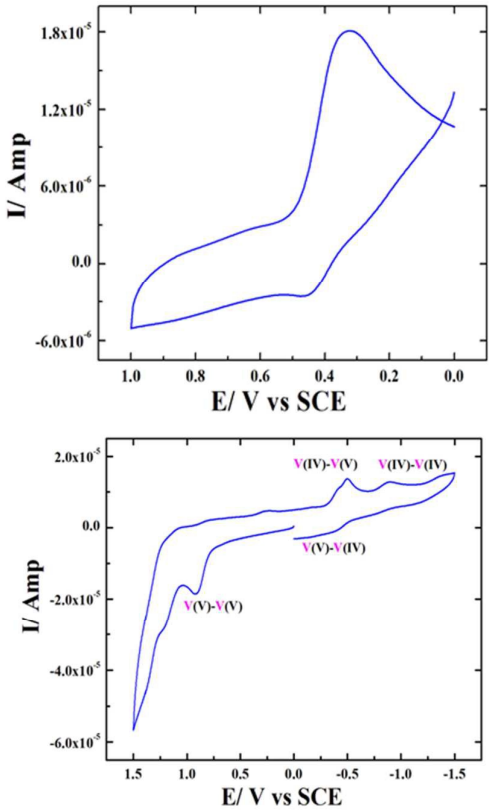

Fig. 4. CV of complexes **1**(above) and **2** (below)in MeCN solvent at 25° C, [C] = 1.0 mM; [TBAPC] = 0.10 M, scan rate = 100 mV s^{-1}.

^{1}H-NMR Studies

The differences between ^{1}H-NMR chemical shifts (Fig. S1, S3 and S6) for free ligand and the complexes **1** and **2** were detected for the atoms near the complexation site. Though there were not so much changes observed in the protons of aromatic region but in case of the protons attached with C7 (3.43 ppm) and C22 (3.56 ppm) for complex **1** appear as triplet and C12 and C16 (3.49-3.80 ppm) for complex **2** appear as multiple signal. However, in case of free ligand these protons appear as singlet at 3.738 ppm (please see the experimental section). Moreover the broad signal of the –OH proton in the free ligand appeared at 9.55 ppm is absent in both the complexes and thus indicates the involvement of it in the complexation and hence stability of the complexes in solution.

Oxidative Bromination of Salicylaldehyde

Many vanadium(V) complexes have been found to catalyze the oxidative bromination of organic substrates in the presence of H_2O_2 and bromide ion[37,38] where vanadium were claimed to be coordinated with one or two equivalents of H_2O_2, forming oxido-monoperoxido, $[VO(O_2)]^+$ and oxido-diperoxido, $[VO(O_2)_2]^-$ species, which ultimately give rise the actual oxidant $[H_2VO_2(O_2)_2]^-$.[39] Then $[H_2VO_2(O_2)_2]^-$ oxidizes bromide ion most likely to HOBr and brominates the substrates. Here complexes **1** and **2** are also found to be able to catalyse the oxidative bromination of salicylaldehyde in the presence of H_2O_2 and bromide ion. During oxidation in acidic medium, one proton coordinates to the oxido group of V=O moiety to form $[(LV=(OH)(Cl]^+$ transiently (**1a**$^+$, Scheme 3) which

Dalton Transactions Accepted Manuscript

View Article Online
CREATED USING THE RSC ARTICLE TEMPLATE - SEE WWW.RSC.ORG/ELECTRONICFILES FOR FURTHER DETAILS DOI: 10.1039/C7DT04718E

Published on 22 January 2018. Downloaded by University of Reading on 24/01/2018 07:27:54.

Table 1.Catalytic parameters for the bromination of salicylaldehyde by KBr/H_2O_2 (KBr = 40 mmol, H_2O_2 = 2 ml i.e. 67 mmol) using complexes **1** and **2** as catalysts (0.04 mmol) in mixed solvents H_2O:MeOH:THF = 4:3:2 at room temperature (25 °C) in presence of 0.2 ml $HClO_4$.

Catalyst	Substrate (mmol)	Reaction time (hr.)	Conversion (%)	%Yield		%Selectivity	TON†
				5-Br-sal (major)	3,5-di-Br-sal		
Complex 1	20	3	11	10	1	90.9	
		6	34	31	3	91.1	
		9	61	54	6	88.5	
		12	81	73	8	90	405
Complex 2	20	3	15	13	2	86.6	
		6	41	36	5	87.8	
		9	69	60	9	86.9	
		12	90	77	13	85.0	450

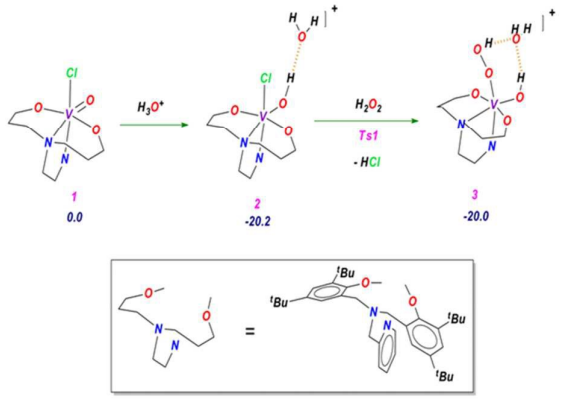

Scheme 3. Schematic representation of intermediates formed during end on hydroperoxido species formation from **1** in the presence of H_2O_2 and H_3O^+. The model form of ligand has been shown in the inset with its original form. In the next schemes we have used this model form of the ligand. Relative free energies of each intermediate are given in kcal/mol.

enhances the electrophilicity of vanadium(V) to facilitate the nucleophilic displacement of Cl^- by H_2O_2 to form aquo-hydroxido-hydroperoxido, $[LV(OH)(OOH)(H_2O)]^+$ (**3**) and then aquo-η^2-peroxido species $[LV(\eta^2\text{-}O_2)(H_2O)]^+$ (**5**, Scheme 5, *vide infra*) which acts as the active intermediate for the catalytic oxidation of Br^- to Br^+ and brominate the substrate.

We have found that $[LV(O)(H_2O_2)]$ (**9**, **Scheme 5**, *vide infra*) formed through the oxidation of Br^- to Br^+ by $[LV(O)(O\cdots Br)(H_3O)]^+$ (**8**) in the presence of H_2O_2/KBr satisfactorily catalyse the oxidative bromination of salicylaldehyde to give 5-bromosalicylaldehyde as a major product along with 3,5-dibromo-salicylaldehyde and 2,3,5-tribromosalicyl-aldehyde as minor products, in the presence of $HClO_4$ in mixed solvents (H_2O:MeOH: THF= 4: 3: 2) at room temperature (*cf.* Scheme 4 and Fig. S10).

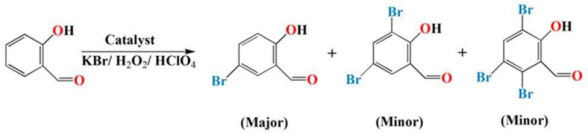

Scheme 4. Formation of different brominated products of salicylaldehyde.

The presence of acid (at least one equivalent of complex) was found to be essential during the catalytic reaction to facilitate the bromination reaction, but excess of $HClO_4$ (>80 mmol) causes decomposition of the catalysts as well as lowering of selectivity of the reaction. In the absence of acid no catalysis was observed. Under the reaction conditions, a maximum of 81% and 90% conversion were achieved with complexes **1** and **2**, respectively within 12 h (Table 1). A plot of % conversion as a function of time (h) gives straight lines for both the complexes (Fig. S11).

In the absence of the catalyst, the reaction mixture gave only 4% conversion of salicylaldehyde to 5-bromosalicylaldehyde. Again, though the conversion of the substrate as well as TON were found to be greater in case of the dimeric complexes than that of the monomeric one, the selectivity is found to be higher in case of the monomeric complex. It may be concluded that the presence of two vanadium(V) unit (in case of dimer, **2**) increases the concentration of the active catalytic species which enhances the conversion of salicylaldehyde to 5-bromosalicylaldeyde and TON.

Kinetic and Mechanistic Studies

We have found that the oxido-vanadium(V) complexes **1** and **2** reported here satisfactorily catalyse the oxidative bromination of salicylaldehyde to give 5-bromosalicylaldehyde as major products using H_2O_2/KBr in the presence of $HClO_4$ in mixed solvents (H_2O:MeOH: THF= 4: 3: 2)[35] at room temp. However, we have carried out all the kinetic studies in pure MeCN.

The reaction was followed by monitoring the visible change in absorbance of the complex at 620 nm. No halogenation of the solvent or ligands has been detected.

Dalton Transactions Accepted Manuscript

View Article Online
CREATED USING THE RSC ARTICLE TEMPLATE - SEE WWW.RSC.ORG/ELECTRONICFILES FOR FURTHER DETAILS DOI: 10.1039/C7DT04718E

Published on 22 January 2018. Downloaded by University of Reading on 24/01/2018 07:27:54.

In the absence of an organic substrate, dioxygen gas was generated upon the addition of one equivalent of hydrogen peroxide to a solution containing the oxidized halide species. Overall, the two reaction steps (Eqn. 2 and 3) correspond to the halide-assisted disproportionation of hydrogen peroxide into water and dioxygen:

$$[L^1V^V(O)Cl] + H^+ \Leftrightarrow [L^1V^V(OH)Cl]^+ \qquad (1)$$

$$[L^1V^V(OH)Cl]^+ + H_2O_2 \Leftrightarrow [L^1V^V(OH)(OOH)]^+ + H^+ + Cl^- \quad (2)$$

$$[L^1V^V(OH)(OOH)]^+ + H_2O_2 \Leftrightarrow [L^1V^V(O)_2]^- + 2H_2O + \frac{1}{2}O_2 \quad (3)$$

Each of these complexes catalyses the bromination of salicylaldehyde in the presence of sufficient equivalents of peroxide, acid, and substrate, performing multiple turn overs in hours at room temperature and milimolar concentrations.

The addition of 1 equivalent $HClO_4$ to an acetonitrile solution of the complex **1** produced observable changes in the UV/visible spectra with a shift in λ_{max} from 619 nm to 765 nm (Figure 5); for complex **1**, shift in λ_{max} occurs from 603 nm to 765 nm, (see Fig. S12 for complex **2**) and may be attributed to the formation of protonated species $[L^1(Cl)V{=}OH]^+$. In contrast, the addition of 10 equivalent of *tert*-butylammonium bromide in the absence of acid produced no observable change in the UV/visible spectra of these complexes.

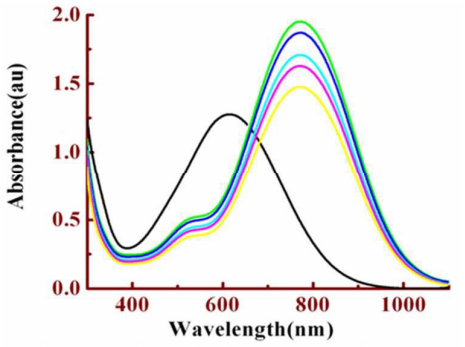

Fig. 5. Shift in λ_{max} of complex **1**(1.0 x 10^{-4} M) with addition of $HClO_4$ (green-yellow curves for 1, 2, 4,6 and 10 equivalents of acid respectively).

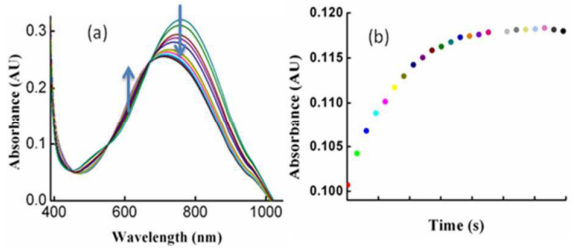

Fig. 6. Time resolved spectra for the catalytic bromination of salicylaldehyde at [**1**] = 1× 10^{-4} M, [Substrate] = 2.5 × 10^{-3} M, [Br^-] = 1.25 × 10^{-3} M and [H_2O_2] = 1.25 × 10^{-3} M showing two clean isosbestic points at 589 and 630 nm; **(b)** corresponding kinetic trace at 620 nm.

The bromide oxidation reaction by **1** is acid catalysed and was confirmed by observing no practical reaction between complex **1** and Br^- in the absence of H^+. It was observed that the rate of reaction increases with the increase in $[H^+]$. However, at high concentration of H^+ (> 0.02M) the complex undergoes rapid decomposition (Fig. S13). Kinetics of the reactions were carried out under pseudo-first-order conditions taking complex as a minor component. The dependence of reaction rates on $[Br^-]$ (1.0 -10 mM) was carried out keeping [C] = 1.0 × 10^{-4} M, $[H^+]$ = 1.25× 10^{-3} M and temperature at 25 °C and monitoring the change in concentration of complex. Kinetic traces are first-order decay

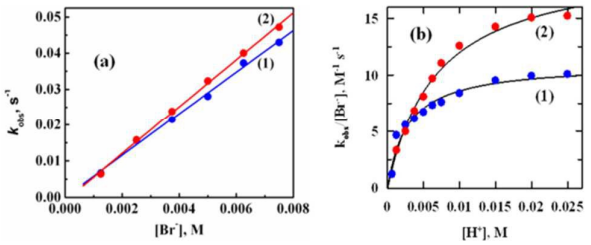

Fig. 7.(a) Variation of rate (k_{obs}) with $[Br^-]$ in MeCN at [**C**] = 1 × 10^{-4} M, [Substrate] = 2.5 × 10^{-3} M, $[H^+]$ = 1.25 × 10^{-3} M and [H_2O_2] = 1.25 × 10^{-3} M; (b) Variation of $k_{obs}/[Br^-]$ with $[H^+]$ in MeCN at [**C**] = 1 × 10^{-4} M, [Substrate] = 2.5 × 10^{-3} M, $[Br^-]$ = 1.25 × 10^{-3} M and [H_2O_2] = 1.25 × 10^{-3} M.

curves at 765 nm while, it is an exponential growth curve at 620 nm (Figure 6b, and Fig. S14 for complex 2) but at both these wavelengths the rate constants evaluated to be almost identical. From the nature of kinetic traces it is obvious that the reaction is first-order dependent on [C] . A plot of k_{obs} (s^{-1}) vs. $[Br^-]$ yields a straight line passing through the origin with slope = k^{Br} = 5.78 ± 0.20 and 6.21 ± 0.13 $M^{-1}s^{-1}$ for complex **1** and **2**, respectively (Figure 7a). Similarly, dependence of rate on $[H^+]$ was carried out keeping $[Br^-]$ = 1.25 × 10^{-3} M and other conditions remaining the same. A plot of k (=$k_{obs}/[Br^-]$) vs. $[H^+]$ gives a non-linear curve of increasing slope (Figure 7b). Non-linear curve-fitting of experimental data to eqn (4) gives K_a = (2.8 ± 0.40) × 10^{-3} and (6.8 ± 0.60) × 10^{-3}; and k^H =(11.01 ± 0.5) and (20.14 ± 0.72) $M^{-1}s^{-1}$ for complex **1** and **2** respectively. Attempts were also taken to determine the thermodynamic acidities of these complexes by monitoring the change in absorbances as a function of $[H^+]$. A plot of absorbance (at 685 nm for **1** and 600 nm for **2**) vs. $[H^+]$ yielded curves of decreasing slopes (Fig. S15) for both the complexes which were solved by adopting eqn 4.[40] It was interesting to note that the evaluated thermodynamic pK_a values (2.34 for **1** and 2.19 for **2**) are in excellent agreement with the kinetic pK_a values (2.55 for **1** and 2.16 for **2**). The reactions were found to be specific acid catalyzed, as the rate constants (k_{obs}, s^{-1}) remain almost constant with the change in concentration of buffer (Cl-AcOH/Cl-AcO$^-$) in the range 0.001-0.01M, at pH 2.93 (Fig. S16).

$$A = \frac{(A_{VH}[H^+] + A_V K_a)}{K_a + [H^+]} \qquad (4)$$

A plausible reaction sequence consistent with the experimental observation may be given by eqns 5-8.

$$VH^+ \overset{K_a}{\leftrightarrow} V + H^+ \qquad (5)$$

$$VH^+ + Br^- \overset{k}{\rightarrow} products \quad (6)$$

$$rate = k[VH^+][Br^-] \quad (7)$$

Dalton Transactions Accepted Manuscript

View Article Online
CREATED USING THE RSC ARTICLE TEMPLATE - SEE WWW.RSC.ORG/ELECTRONICFILES FOR FURTHER DETAILS DOI: 10.1039/C7DT04718E

Published on 22 January 2018. Downloaded by University of Reading on 24/01/2018 07:27:54.

$$k_{obs} = \frac{k[H^+][Br^-]}{K_a + [H^+]} \qquad (8)$$

$$[L^1V^V(OH)(OOH)]^+ + Br^- \leftrightarrows [L^1V^V(O)_2]^- + H_2O + Br^+ \qquad (9)$$

$$RH + Br^+ \leftrightarrows RBr + H^+ \qquad (10)$$

$$[L^1V^V(O)_2]^- + H_2O_2 + 2H^+ \leftrightarrows [L^1V^V(OH)(OOH)]^+ + H_2O \qquad (11)$$

$$RH + H_2O_2 + Br^- + H^+ \rightarrow RBr + 2H_2O \qquad (12)$$

In the presence of multiple equivalents of H_2O_2, bromide and H^+ the vanadium complexes act as catalyst for the peroxidative halogenation of salicylaldehyde. Under this catalytic conditions (H_2O_2/KBr 500 equivalent each with respect to catalyst in mixed solvents H_2O:MeOH:THF=4: 3:2 in the presence of $HClO_4$ at room temperature) bromination of salicylaldehyde occurs within 12 h with TON 405 and 450 for complexes **1** and **2**, respectively. The catalytic bromination of salicylaldehyde can be rationalized by adopting the reaction sequences (9-12) together with eqns. 1 and 2.

Our complex **1** initially turns into $[L^1V(OH)(OOH)(H_2O)]^+$ (**3**) (Fig. S17) which ultimately turns to $[LV(O)(O_2H_2)]$ (**9**) through oxidation of Br^- to Br^+. $[L^1V(O)_2]$ regenerates the catalyst $[L^1V(OH)(OOH)\text{-}(H_2O)]^+$ (**3**) by reaction with H_2O_2 in the presence of acid. The overall reaction involves one mole of substrate (RH), one mole H_2O_2 and one mole of Br^- and in presence two equivalents of H^+ to form one mole of product and water.

Computational Studies

Recently Pecoraro and coworkers have theoretically investigated the for vanadium haloperoxidase catalysed Br^- oxidation process.[41] They have shown that the epical hydroxyl group present in the active site of vanadium haloperoxidase is activated by a histidine residue via hydrogen bonding, which triggers the proton abstraction from H_2O_2 and subsequent end-on (EO) hydroperoxido species formation after H_2O release. In the next step EO hydroperoxido species is converted to side-on (EE) peroxido form after release of another water molecule. After that bromide anion performs a nucleophilic attack to the side on peroxido species $[V(O_2)]$ to yield V(O)(OX), which after protonation releases HOX. So the side-on peroxido species formation from H_2O_2 is crucial for oxidation of halide ion in the case of haloperoxide enzymes. In this work, we have investigated the side-on peroxido species formation from our model catalyst (**1**) of vanadium haloperoxidase in the presence of H_2O_2 and H_3O^+ and subsequently HOBr formation from Br^- with the assistance from the side on peroxido species.

At first, we have optimized the parent mononuclear oxidovanadium complex (**1**) using DFT (see Fig.8). We have found that V-O3 and V-N1 bond distances are 1.58 and 2.20 Å, respectively which are almost similar with the crystallographic values (V-O3 = 1.589 and V-N1= 2.157 Å). So our used theoretical method predicted the geometry of the catalyst reasonably well, which provides justification of our used theoretical approach.

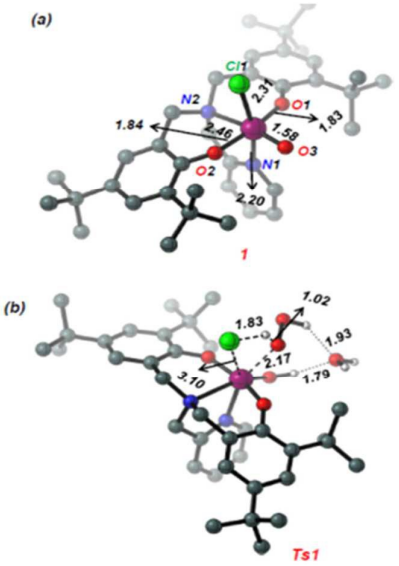

Fig.8. Optimized structure of (a) oxido-vanadium catalyst (**1**) and (b) transition state (**Ts1**) for apical end on hydroperoxido complex formation via HCl elimination. All bond lengths are in the unit of Å.

Kinetic and mechanistic studies on the model catalyst (**1**) suggested that protonation of V=O bond present in oxido-vanadium complex is happening at the initial stage of the catalytic cycle. So, first we have calculated the thermodynamic preference of the protonation step of catalyst **1** (see Scheme 3). We have used H_3O^+ to account for the presence of acid as the strong perchloric acid will be ionized in the presence of water.

Our theoretical calculation revealed that the formation of protonated oxido-vanadium complex (**2**) from **1** and H_3O^+ is a highly exothermic process (ΔG = -20.2 kcal/mol) (see Scheme 1). After protonation **1a**$^+$, a hydrogen bonded complex of V-OH moiety and H_2O, is obtained. In the next step, we have found that in the presence of H_2O_2, V-Cl bond (present in **1a**$^+$) is broken and V-OOH bond is formed simultaneously along with the release of HCl. The whole process has occurred through **Ts1** (shown in Fig.8) by overcoming free energy activation barrier of 18.2 kcal/mol. The formation of **3** (shown in Scheme 3) with end on peroxo moiety and free HCl from **1a**$^+$ and H_2O_2 is almost a thermo neutral process in terms of free energy (ΔG = 0.2 kcal/mol).

In the following section, we have explored the formation of side-on peroxido species from **3**. We have found that end on hydroperoxido form (**3**) can isomerizes to side on hydroperoxido form (**4**), where both the peroxido oxygen atoms are coordinated to the vanadium center (shown in Fig.9 and Scheme 5).

Dalton Transactions Accepted Manuscript

View Article Online
CREATED USING THE RSC ARTICLE TEMPLATE - SEE WWW.RSC.ORG/ELECTRONICFILES FOR FURTHER DETAILS DOI: 10.1039/C7DT04718E

Published on 22 January 2018. Downloaded by University of Reading on 24/01/2018 07:27:54.

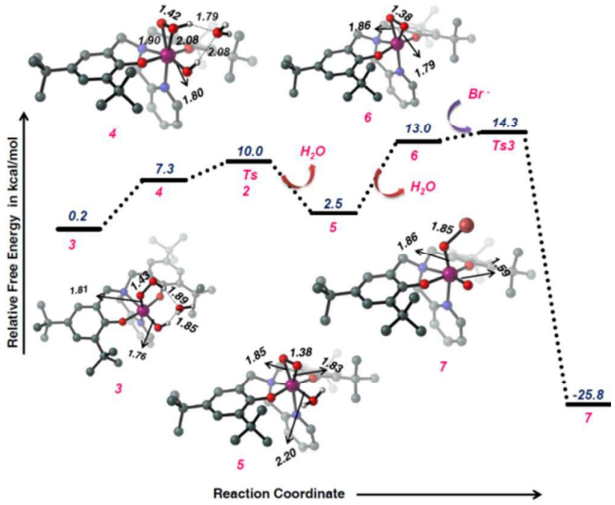

Fig.9. Relative free energy profile for side-on peroxidoo (6) formation from 3 and subsequent oxidation of Br- to yield –OBr¯. Optimized geometries of intermediates along the reaction path have been included in the Figure. All bond lengths are in Å.

Formation of **4** is endoergic by 7.30 kcal/mol with respect to **3** in terms of free energy. In case of vanadium halopeoxidase a water molecule is present near the metal cofactor similar to **4**. Later on Pecoraro and De Gioia have shown that this water molecule act as a proton shuttle to relay the proton present in metal bound end on hydroperoxido to equatorial hydroxyl group, which has low activation barrier compared to direct proton transfer.[42] Similarly, we have found that **4** is transformed to **5** through **Ts2**, where additional water molecule present near side-on hydroperoxido moiety present in **4** act as a proton shuttle (see Fig. 10). The free energy activation barrier of **Ts2** is 10.0 kcal/mol and formation of **5** and free H_2O from **4** is exoergic by 5.0 kcal/mol.

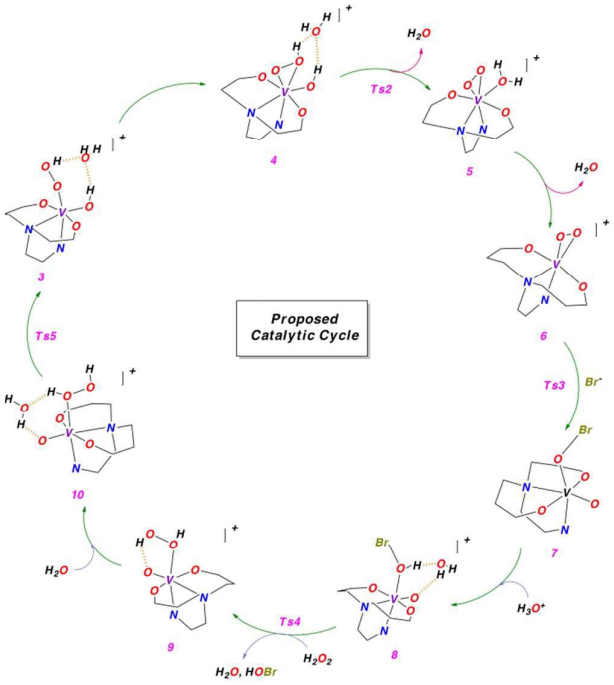

Scheme 5. Schematic representation of the full catalytic cycle where **3** act as an catalytic species and oxidized Br- to BrO- in presence of H_2O_2 and H_3O^+.

Starting with **5**, we have found that it can be converted to **6** via dissociation of equatorial water molecule in expense of 13.0 kcal/mol. After that Br^- anion performs a nucleophilic attack to the one of the side-on peroxido atom from the apical side opposite to the pyridine ligand.

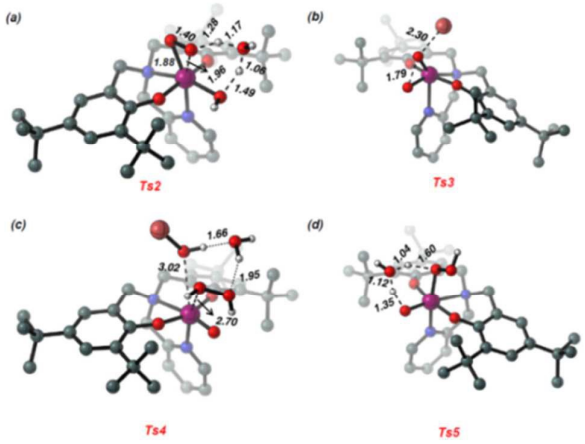

Fig.10. Optimized geometries of transition state for (a) water assisted proton relay to produce end-on peroxido formation from end on hydroperoxido species (**Ts2**), (b) nucleophilic attack of Br^- to end-on peroxido species (**Ts3**), (c) release of HOBr from the apical site of the metal center in the presence of H_2O_2 (**Ts4**) and (d) proton relay from metal bound H_2O_2 to equatorial V-O bond with the help of water molecule (**Ts5**). All bond lengths are in Å.

The free energy activation barrier of the peroxido cleavage transition state (**Ts3**) (see Fig. 10) by the Br^- anion is 14.3 kcal/mol. As a results of peroxido cleavage, **7** (see Fig. 9) is formed having an epical V-OBr and equatorial V-O and formation of **7** is highly exoergic process (ΔG = -25.8 kcal/mol). **7** can transform into **8** (see Fig 11 and Scheme 6) after protonation of the epical -OBr group with the help of H_3O^+, which is also a highly exoergic process (ΔG = -30.2 kcal/mol). We have also seen the possibility of protonation of equatorial V-O bond in the presence of H_3O^+, but it is endoergic by 2.6 kcal/mol compared to V-OBr protonation process. Another equivalent of H_2O_2 can displace the metal bound epical HOBr along with H_2O molecule hydrogen bonded with it through **Ts4** (see Fig. 10) having free energy activation barrier of 10.2 kcal/mol with respect to **8**. As a result of H_2O_2 assisted displacement of HOBr hydrogen bonded with H_2O, **9** (see Fig. 11 and scheme 6) is formed where the metal center contains an epical hydroperoxido group which is hydrogen bonded with the equatorial metal oxo group and formation of **9** is endoergic by 10.5 kcal/mol in terms of free energy. After that a water molecule can bind between the hydroperoxido and oxido group to assist the proton transfer from V(OH-OH) to V-O center.
Formation of hydrogen bonded intermediate **10** (see Fig.11 and scheme 6) is favore by 5.7 kcal/mol compared to **9** and free H_2O molecule. After proton relay from V(HO-OH) moiety to V-O moiety via **Ts5** (see Fig.10) with the help of proton shuttle H_2O molecule by climbing free energy activation barrier of 12.4 kcal/mol **3** is regenerated. Formation of **3** is

Dalton Transactions Accepted Manuscript

View Article Online
CREATED USING THE RSC ARTICLE TEMPLATE - SEE WWW.RSC.ORG/ELECTRONICFILES FOR FURTHER DETAILS DOI: 10.1039/C7DT04718E

Published on 22 January 2018. Downloaded by University of Reading on 24/01/2018 07:27:54.

endoenergic by 4.8 kcal/mol compared to **8** which is the most stable intermediate of the catalytic cycle.

Despite the endoergic nature of the catalytic cycle, the oxidation of Br^- will be a spontaneous process as it is coupled with bromination of salicylaldehyde, which is a highly exoergic process (ΔG = -44.3 kcal/ mol). Possible intermediates of the bromination of salicylaldehyde by the protonated HOBr have been shown in Scheme 6. So our detail theoretical calculation suggests that **3** is the active catalytic species.

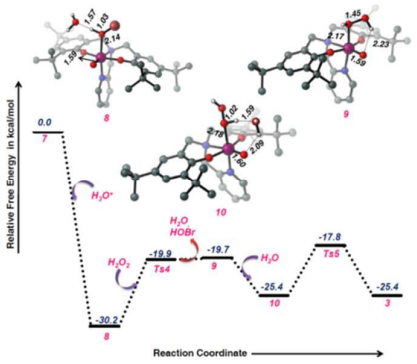

Fig.11. Relative free energy profile for regeneration of catalytic species **3** from **7** in presence of H_3O^+ and H_2O_2. Optimized geometries of intermediates along the reaction path have been included in the figure. All bond lengths are in Å.

So our mechanistic investigation about the catalytic cycle for bromination of salicylaldehyde using Br^- anion, H_2O_2 and H_3O^+ in the presence of catalyst **1** shows that the whole catalysis has three parts: (i) active catalytic species (**3**) formation from **1** in the presence of H_3O^+ and H_2O_2, (ii) oxidation of Br^- anion to HOBr via side on peroxo formation and (iii) bromination of salicylaldehyde by protonated HOBr. The rate determining step of the whole catalytic cycle is **Ts3**, where O-O bond of side on peroxo species is broken by the nucleophilic attack of Br^- anion, having a free energy activation barrier of 14.3 kcal/mol.

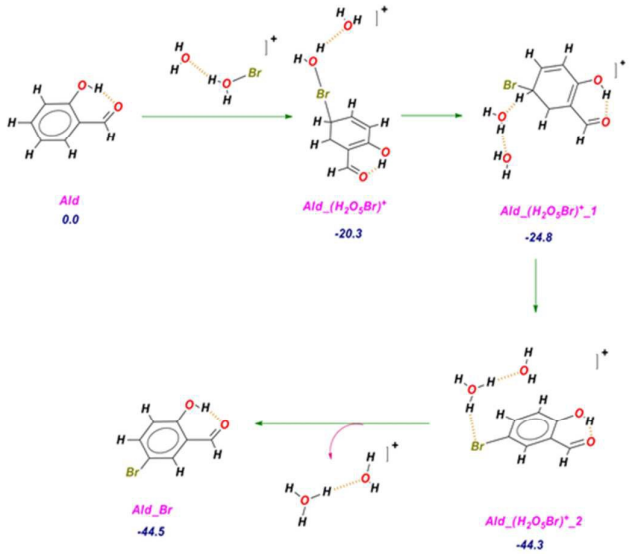

Scheme 6. Schematic representation of the intermediates formed during the bromination of salicylaldehyde using $[HOBr.H_3O]^+$. salicylaldehyde, sigma complex after addition of Br^+ to the para position of aromatic ring of salicylaldehyde (with respect to OH group) where one water molecule coordinating to Br, sigma complex where acidic para hydrogen is hydrogen bonded with water molecule, brominated salicylaldehyde hydrogen bonded with $H_2O_5^+$ via Br-H hydrogen bond. Borominated salicylaldehyde is abriviated as Ald, $Ald\_(H_2O_5Br)^+$, $Ald\_(H_2O_5Br)^+\_1$, $Ald\_(H_2O_5Br)^+\_2$ and Ald_Br. Relative free energies of each intermediates are given in kcal/mol.

Conclusion

The mono nuclear $[V^{V}O(L^1)(Cl)]$ (**1**) and dinuclear $[L^1V^{V}O(\mu_2\text{-}O)VO(L^1)]$ (**2**) oxido-vanadium(V) complexes of a ONNO donor amine-*bis*(phenolate) ligand (H_2L^1) have been characterized by mass spectroscopy,^{1}H-NMR and FTIR study. Both the complexes possess distorted octahedral geometry around the V centers. The complexes **1** and **2** are efficient to catalyze the oxidative bromination of salicylaldehyde in the presence of H_2O_2 to produce 5-bromo salicylaldehyde as the major product with TONs 405 and 450, respectively in mixed solvent (H_2O: MeOH: THF = 4: 3: 2). On the addition of 1 equivalent or more acid to MeCN solution of complex **1,** it immediately turned into their protonated forms with the shift in λ_{max} from 610 nm to 765 nm. Analogous shift in λ_{max} was observed in the case of complex **2**. The kinetic analysis of the bromide oxidation reaction indicates a mechanism which is first order in protonated peroxido-vanadium complex and bromide ion and limiting first-order on $[H^+]$. The evaluated k^{Br} and k^{H} values are 5.78 ± 0.20 and 11.01 ± 0.50 M^{-1} s^{-1} for complex **1** and 6.21 ± 0.13 and 20.14 ± 0.72 $M^{-1}s^{-1}$ for complex **2**, respectively with corresponding pK_a values of 2.55 and 2.17. The corresponding thermodynamic pK_a values, determined by monitoring absorbances as a function of $[H^+]$, are in well agreement with the kinetic pK_a values. Our mechanistic investigation for bromination of salicylaldehyde in th presence of catalyst **1** involves Br^- anion, H_2O_2 and H_3O^+ and the whole catalytic process consists of: (i) formation of active catalytic species (**3**) from **1** in presence of H_3O^+ and H_2O_2, (ii) oxidation of Br^- anion to HOBr via formation of side on peroxido species and

Dalton Transactions Accepted Manuscript

View Article Online
CREATED USING THE RSC ARTICLE TEMPLATE - SEE WWW.RSC.ORG/ELECTRONICFILES FOR FURTHER DETAILS DOI: 10.1039/C7DT04718E

Published on 22 January 2018. Downloaded by University of Reading on 24/01/2018 07:27:54.

finally (iii) bromination of salicylaldehyde by protonated HOBr. The rate determining step of the whole catalytic cycle is **Ts3**, where O-O bond of side-on peroxo species is broken by the nucleophilic attack of Br^-, with free energy activation barrier of 14.3 kcal/mol.

Acknowledgement
Financial supports from DST West Bengal (809(Samc)/ST/P/S&T/4G-9/2014) is gratefully acknowledged.

†Electronic supplementary information (ESI) available. For ESI and crystallographic data in CIF or other electronic format see DOI: 10.1039/

References

1 D. Rehder, *Angew. Chem., Int. Ed. Engl.*,1991, **30**, 148-167.
2 (a) Y. Shechter, S. J. D. Karlish, *Nature*, 1980, **284**, 556-558; (b) J. H. McNeill, V. G. Yuen, H. R. Hoveyda, C. Orvig, *J. Med. Chem.*,1992, **35**, 1489-1491.
3 R. Wever, *Nature*, 1988, **335**, 501.
4 P. M. Gschwend, J. K. MacFarlane, K. A. Newman, *Science*, 1985, **227**, 1033-1035.
5 A. Butler, J.V. Walker, *Chem. Rev*. 1993, **93**, 1937-1944.
6 A. Butler, *Coord. Chem. Rev*. 1999, **187**, 17-35.
7 R. R. Everett, J. R. Everett, A. Kanofsky, A. Butler, *J. Biol. Chem*., 1990, **265**, 4908-4914.
8 A. Butler, in: J. Reedijk, E. Bouwman (Eds.), *Bioinorganic Catalysis*, 2nd ed (Chapter 5), Marcel Dekker, New York, 1999.
9 R. R. Everett, A. Butler, *Inorg. Chem.*,1989, **28**, 393-395.
10 R. R. Everett, H. S. Soedjak, A. Butler, *J. Biol. Chem.* 1990, **265**, 15671-15679.
11 R. A. Tschirret-Guth, A. Butler, *J.Am. Chem. Soc.*,1994, **116**, 411-412.
12 (a) R. Wever, E. de Boer, B.E. Krenn, H. Offenberg, H. Plat, *Prog.Clin. Biol. Res*., 1988, **274**, 477; (b) R. Wever, W. Hemrika, in: J.O. Nriagu (Ed.), *Vanadium in the Environment. Part 1:Chemistry and Biochemistry*, *Wiley*, New York, 1997, pp 285.
13 D. Rehder, *Coord. Chem. Rev*., 1999, **182**, 297-322.
14 D. Rehder, C. Schulzke, H. Dau, C. Meinke, J. Hanss, M. Epple, *J. Inorg. Biochem*., 2000, **80**, 115-127.
15 D. C. Crans, A. D. Keramidas, S. S. Amin, O. P. Anderson, S. M. Miller, *J. Chem. Soc. Dalton Trans*., 1997, **16**, 2799-2812.
16 M. Mahroof-Tahir, A. D. Keramidas, R. B. Goldfarb, O. P. Anderson, M. M. Miller, D. C. Crans, *Inorg. Chem*., 1997, **36**, 1657-1668.
17 M. Bashirpoor, H. Schmidt, C. Schulzke, D. Rehder, *Chem. Ber./Recueil*., 1997, **130**, 651-657.
18 W. Z. Plass, *Anorg. Allg. Chem*., 1997, **623**, 461.
19 R. Fulwood, H. Schmidt, D. Rehder, *J. Chem. Soc. Chem. Commun*., 1995, **12**, 1443-1444.
20 N. Julien-Cailhol, E. Rose, J. Vaisserman, D. Rehder, *J. Chem. Soc. Dalton Trans*., 1996, **10**, 2111-2115.
21 V. Vergopoulos, W. Priebsch, M. Fritzsche, D. Rehder, *Inorg. Chem*., 1993, **32**, 1844-1857.
22 R. De La Rose, M. J. Clague, A. Butler, *J. Am. Chem. Soc*., 1992, **114**, 760-761.
23 F. Secco, *Inorg. Chem*., 1980, **19**, 2722-2725.
24 D. Maity, A. Ray, W. S. Sheldrick, H. M. Figge, B. Bandyopadhyay, M. Ali, *Inorg. Chim. Acta*, 2006, **359**, 3197-3204.
25 D. Maity, J. Marek, W. S. Sheldrick, H. Mayer-Figge, M. Ali, *J. Mol. Catal. A: Chem*., 2007, **270**, 153-159.
26 D. Maity, M. Mijanuddin, M. G. B. Drew, J. Marek, P. C. Mondal, B. Pahari, M. Ali, *Polyhedron*, 2007, **26**, 4494-4502.
27 M. Debnath, A. Dutta, S. Biswas, K. K. Das, H. M. Lee, J. Vícha, R. Marek, J. Marek, M. Ali, *Polyhedron*, 2013, **63**, 189-198.
28 M. J. Frisch, G. W. Trucks, H. B. Schlegel, G. E. Scuseria,M. A. Robb, J. R. Cheeseman, G. Scalmani, V. Barone,B. Mennucci, G. A. Petersson, H. Nakatsuji, M. Caricato,X. Li, H. P. Hratchian, A. F. Izmaylov, J. Bloino, G. Zheng,J. L. Sonnenberg, M. Hada, M. Ehara, K. Toyota,R. Fukuda, J. Hasegawa, M. Ishida, T. Nakajima, Y. Honda,O. Kitao, H. Nakai, T. Vreven, J. A. Montgomery Jr,J. E. Peralta, F. Ogliaro, M. Bearpark, J. J. Heyd,E. Brothers, K. N. Kudin, V. N. Staroverov, R. Kobayashi,J. Normand, K. Raghavachari, A. Rendell, J. C. Burant,S. S. Iyengar, J. Tomasi, M. Cossi, N. Rega, J. M. Millam,M. Klene, J. E. Knox, J. B. Cross, V. Bakken, C. Adamo,J. Jaramillo, R. Gomperts, R. E. Stratmann, O. Yazyev,A. J. Austin, R. Cammi, C. Pomelli, J. W. Ochterski,R. L. Martin, K. Morokuma, V. G. Zakrzewski, G. A. Voth,P. Salvador, J. J. Dannenberg, S. Dapprich, A. D. Daniels, Ö. Farkas, J. B. Foresman, J. V. Ortiz, J. Cioslowski andD. J. Fox, *Gaussian 09, Revision A.1, Gaussian, Inc.,* Wallingford, CT, 2009.
29 A. D. Becke, *J. Chem. Phys*., 1993, **98**, 5648.
30 Marenich, A. V.; Cramer, C. J.; Truhlar, D. G. J. Phys. Chem. B 2009, 113, 6378−6396.
31 Wertz, D. H. J. Am. Chem. Soc. 1980, 102, 5316−5322.
32 (a) Li, H.; Wang, X.; Huang, F.; Lu, G.; Jiang, J.; Wang, Z.-X. Organometallics 2011, 30, 5233−5247. (b) Yu, Z.-X.; Houk, K. N. J. Am. Chem. Soc. 2003, 125, 13825−13830. (c) Li, H.; Wang, X.; Wen, M.; Wang, Z.-X. Eur. J. Inorg. Chem. 2012, 5011−5020. (d) Li, H.; Wen, M.; Wang, Z.-X. Inorg. Chem. 2012, 51, 5716−5727. (e) Zhao, L.; Huang, F.; Lu, G.; Wang, Z.-X.; Schleyer, P. v. R. J. Am. Chem. Soc. 2012, 134, 8856−8868. (f) Qu, S.; Dang, Y.; Song, C.; Wen, M.; Huang, K.-W.; Wang, Z.-X. J. Am. Chem. Soc. 2014, 136, 4974−499. (g) Ding, L.; Ishida, N.; Murakami, M.; Morokuma, K. J. Am. Chem. Soc. 2014, 136, 169−178.
33 E. Y. Tshuva, I. Goldberg, M. Kol, *Organometallics,* 2001, **20**, 3017-3028.
34 G. M. Sheldrick, Acta Crystallogr., Sect. A: Fundam. Crystallogr., 2014, 64, 112.
35 B.F. Sels, D. E. De Vos, M. P. Buntinx, A. Jacobs, *J. Catal*., 2003, **216**, 288-297.
36 (a) T. K. Paine, T. Weyhermüller, E. Bill, E. Bothe, P. Chaudhuri, *Eur. J. Inorg. Chem*., 2003, **24**, 4299-4307; (b) G. Asgedom, A. Sreedhara, C. P. Rao, *Polyhedron*, 1995, **14**, 1873-1879; (c) G. Asgedom, A. Sreedhara, J. Kivikoski, J. Valkonen, E. Kolehmainen C. P. Rao, *Inorg. Chem*., 1996, **35**, 5674-5683.
37 J. A. Martinez-Perez, M. A. Pickel, E. Caroff, W. D. Woggon, *Synlett*., 1999, **12**, 1875-1878.
38 C. L. Perrin, T. J. Dwyer, *Chem. Rev*., 1990, **90**, 935-967.
39 A. G. J. Ligtenbarg, R. Hage, B. L. Feringa, *Coord. Chem. Rev*., 2003, **237**, 89-101.
40 (a) C. F. Bernasconi, Ali, M.; Gunter, J. C. Kinetic and *J. Am. Chem. Soc.* 2003, **125**, 151–157 (b) Bernasconi, C. F.; Ali, M.; Lu, F. *J. Am. Chem. Soc*. 2000, **122**, 1352–1359.
41 G. J. Colpas, B. J. Hamstra, J. W. Kampf, V. L. Pecoraro, *J. Am. Chem. Soc.*, 1996, **118**, 3469-3478.
42 Zampella, G.; Fantucci, P.; Pecoraro, V. L.; Gioia, L. D. *Inorg. Chem.* 2006, 45, 7133-7143.

Dalton Transactions Accepted Manuscript

View Article Online
CREATED USING THE RSC ARTICLE TEMPLATE - SEE WWW.RSC.ORG/ELECTRONICFILES FOR FURTHER DETAILS DOI: 10.1039/C7DT04718E

Published on 22 January 2018. Downloaded by University of Reading on 24/01/2018 07:27:54.

Dalton Transactions Accepted Manuscript